IOPscience iopscience.iop.org

Home Search Collections Journals About Contact us My IOPscience

Comparison of different spectroscopic techniques for detection of excitons

This article has been downloaded from IOPscience. Please scroll down to see the full text article.

2000 J. Phys.: Condens. Matter 12 1111

(http://iopscience.iop.org/0953-8984/12/6/327)

View the table of contents for this issue, or go to the journal homepage for more

Download details:
IP Address: 171.66.16.218
The article was downloaded on 15/05/2010 at 19:54

Please note that terms and conditions apply.

J. Phys.: Condens. Matter **12** (2000) 1111–1117. Printed in the UK PII: S0953-8984(00)05810-0

Comparison of different spectroscopic techniques for detection of excitons

V Sh Machavariani

Raymond and Beverly Sackler School of Physics and Astronomy, Tel-Aviv University, Ramat-Aviv, 69978, Israel

Received 28 July 1999, in final form 18 October 1999

Abstract. Requirements on the energy resolution for the detection of an exciton by the x-ray transmission, fluorescence, photocurrent and reflectivity techniques have been considered. X-ray reflectivity appears to be the most suitable technique for exciton detection. An excitonic origin of the narrow peak in the Si $L_{2,3}$ reflectivity spectrum is suggested.

1. Introduction

Excitons, or localized electronic states with energy smaller than the band gap, might appear because of a core-hole potential. The hole appears in the final state of the x-ray absorption process or in the intermediate state of the fluorescence and elastic scattering processes. The enhancement just above the threshold in the crystalline silicon x-ray absorption spectrum was explained for the first time by Altarelli and Dexter [1] in terms of the Elliott [2] exciton in 1972. The problem of the exciton in the Si $L_{2,3}$ absorption edge was thoroughly studied [3–6]. Nevertheless, up to now this problem remains under consideration [7–9]. The excitons have some peculiar properties which make it difficult to detect them by x-ray absorption spectroscopy. First of all, the excitonic peak appears in the absorption spectrum near the absorption threshold (the bottom of the conduction band). The energy gap between them is very small. Thus, the excitonic peak appears in the region of the sharp increase of the absorption cross section. The second problem is that the excitonic peak has rather a small integral intensity [10]. The only opportunity to detect it is connected with its extremely narrow width. Due to this sharpness, it is possible to distinguish between the excitonic peak and the conduction band.

In this paper we compare the requirements on the energy resolution of the experimental set-up for the detection of the excitonic peaks in the x-ray absorption, fluorescence, photocurrent and reflectivity techniques. We will show that the reflectivity technique seems to be the most favourable for exciton detection. In section 2 the energy resolution for the detection of the narrow peak using the transmission, fluorescence and photocurrent techniques will be briefly discussed. In section 3 we will consider the reflectivity spectrum for large glancing angle and show the difference between the contributions of the excitons to the reflectivity and absorption spectra. In section 4 the calculation of the permittivity in Si crystal is presented. The excitonic origin of a sharp narrow peak in the XRFS spectrum [11, 12] of Si crystal is considered. The conclusions are presented in section 5.

0953-8984/00/061111+07$30.00 © 2000 IOP Publishing Ltd

2. Transmission, fluorescence and photocurrent techniques

It is widely assumed that two peaks in the x-ray absorption fine-structure spectrum (XAFS) are distinguishable if the distance between them ΔE is larger than the energy width of the apparatus function Γ_0. This assumption appears from the result of the convolution of the absorption coefficient spectrum $\mu(E)$ with the apparatus function.

But in the transmission experiment the experimental energy broadening influences not the absorption coefficient μ itself but the ratio of transmitted to incident radiation intensities I_1/I_0. One needs to convolute with the energy apparatus function not the absorption coefficient μ but the ratio I_1/I_0, because the very value I_1/I_0 is measured in the transmission experiment. The difference between these two types of averaging becomes important if the peak intensity sufficiently exceeds the background absorption:

$$\Delta\mu\, x \gg \mu_0 x \tag{1}$$

where x is the thickness of the sample and $\Delta\mu$ is the difference between the peak intensity and the background μ_0. It is important to note here that this is exactly the case for the excitons. While the integral intensity of the excitonic peak is rather small, the peak value sufficiently exceeds the background absorption because of its extremely small width. In this case the peak width itself becomes important, but not the distance to the next peak.

Let us consider the peak of the width Γ_{ex} in $\mu(E)$ centred near the energy E_0. The peak value $\mu(E_0)$ is much greater than the background absorption. In this case the ratio I_1/I_0 has a sharp minimum of the width Γ_{ex} near the energy E_0. The value of this ratio around E_0 is practically zero. However, as a result of the experimental energy broadening, instead of zero transmitted intensity one obtains the final value which is determined not by the distance to the other peaks but by the ratio of the width of the peak Γ_{ex} to the apparatus energy width Γ_0. Even a small additional signal resulting from the non-monochromaticity of the radiation increases this ratio by many times. Thus the experimentally obtained absorption coefficient $\mu_{exp}(E_0) \propto -\ln(I_1/I_0)$ drops down by many times in comparison with the real $\mu(E_0)$. The peak might even disappear.

Figure 1 presents the absorption coefficient of Si crystal near the Si $L_{2,3}$ absorption edge. The details of the permittivity calculation are presented in section 4. The left (a) and right (b) parts of figure 1 correspond to the widths of the apparatus function, which are 0.1 eV and 0.2 eV respectively. The upper curves correspond to the convolution of the absorption coefficient with the energy apparatus function. To obtain the second and the third (going from top to bottom) curves we first calculated the ratio $I_1/I_0 = \exp(-\mu x)$. After this we convoluted the ratio I_1/I_0 with the Lorentz function

$$f(E) = \frac{1}{\pi}\int \frac{I_1(E_0)}{I_0(E_0)} \frac{\Gamma_0/2}{(E-E_0)^2 + \Gamma_0^2/4}\,\mathrm{d}E_0 \tag{2}$$

and found the 'experimentally' measured value of $\mu_{exp}(E) = -(\ln f(E))/x$. These curves have been calculated for thicknesses of the sample of 50 and 100 Å respectively. These thicknesses correspond to $\mu x \approx 0.5$ and $\mu x \approx 1$ respectively at the energy 102 eV. One can see from figure 1 that the smaller the thickness of the sample, the easier the detection of the excitonic peak.

The fluorescence technique is also limited for the exciton detection because of the self-absorption. If the peak value sufficiently exceeds the background absorption then its amplitude (and integral intensity) is drastically decreased by the self-absorption. In this case the smoothing because of the apparatus energy width could make the peak indistinguishable. To correct the fluorescence spectrum one needs first to deconvolute it. While for the usual spectrum the difference between the deconvoluted and non-deconvoluted experimental spectra

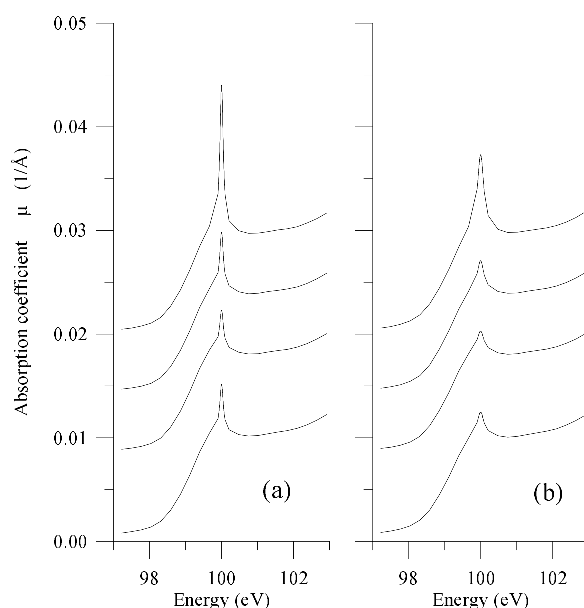

Figure 1. The convoluted absorption coefficient (upper curves) for Si crystal near the Si $L_{2,3}$ absorption edge. The second and third curves (going from top to bottom) correspond to the absorption coefficient from the transmission technique for thicknesses of the sample of 50 and 100 Å respectively. The lowest curves correspond to the fluorescence corrected for the self-absorption. The widths of the apparatus function are 0.1 eV (a) and 0.2 eV (b). For clarity the curves are shifted.

is small, in the case of the presence of excitons this difference becomes crucial because of the large ratio of the apparatus width to the excitonic peak width.

The lowest curves in figure 1 show the calculated fluorescence spectra, which were convoluted with the Lorentz apparatus function and, after this, corrected for self-absorption. The glancing angle of the incident radiation is 45°; the emitted radiation (the radiation transition from the Si 3s to 2p levels, $\hbar\omega \approx 85$ eV) is detected in the direction perpendicular to the surface. The vertical scales for the lowest curves are arbitrary. One can see that it is difficult to detect the excitonic peak by the fluorescence technique.

The techniques involving the measurement of the photocurrent or Auger electrons [13, 14] might be more profitable for detection of the excitonic peak, because in this case the experimental spectrum is proportional to the absorption cross section. In this case the absorption coefficient itself is convoluted with the apparatus function. One can see from figure 1 (upper curves) that the excitonic peak is much more distinguishable in this case.

3. Reflectivity

In this paper we suggest using the XRFS spectrum for the detection of the narrow (excitonic) peaks. If the glancing angle $\Theta \gg \Theta^{\rm crit}$, the reflectivity R has the form (according to the Fresnel formulae [15]) $R = (\alpha^2 + \beta^2)/(16 \sin^4 \Theta)$, where $\Theta^{\rm crit}$ is the critical angle of the total external reflection, $\Theta^{\rm crit} = \sqrt{\alpha}$, and $\varepsilon = 1 - \alpha + {\rm i}\beta$, where ε is the permittivity of the crystal. Because of the Kramers–Kronig relation [15] between the real and imaginary parts of the permittivity, α is not arbitrary but is determined by β. The peak of the width Γ and the integral intensity A

in the imaginary part of the permittivity could be written as follows:

$$\beta(E) = \frac{A}{\pi}\left(\frac{\Gamma/2}{(E_0 - E)^2 + \Gamma^2/4} - \frac{\Gamma/2}{(E_0 + E)^2 + \Gamma^2/4}\right) \tag{3}$$

where E_0 is the energy of the centre of the peak. In this case α has the form

$$\alpha(E) = \frac{A}{\pi}\left(\frac{E_0 - E}{(E_0 - E)^2 + \Gamma^2/4} + \frac{E_0 + E}{(E_0 + E)^2 + \Gamma^2/4}\right). \tag{4}$$

In the close vicinity of E_0 the reflectivity has the form $R \propto A^2/[(E_0 - E)^2 + \Gamma^2/4]$, where we have neglected the contribution from the parts with the sum $E_0 + E$ in the denominator. Thus in the reflectivity spectrum ($\Theta \gg \Theta^{crit}$) there is a peak at the same position E_0 and with the same width Γ as in the absorption. Therefore the reflectivity spectrum for $\Theta \gg \Theta^{crit}$ seems to be proportional to the absorption one. But the peak in the reflectivity spectrum has a different integral intensity, A^2/Γ. The narrower the peak in the absorption spectrum, the larger its integral intensity in the reflectivity spectrum. Comparison of the reflectivity and absorption spectra of two narrow peaks with the widths Γ_1 and Γ_2 allows us to find the ratio of their widths Γ_1/Γ_2 even in the case of large experimental broadening (until this broadening does not change the integral intensities of the peaks):

$$\frac{\Gamma_1}{\Gamma_2} = \frac{A_2^{refl}}{A_1^{refl}}\left(\frac{A_1^{abs}}{A_2^{abs}}\right)^2 \tag{5}$$

where A^{abs} and A^{refl} are the integral intensities of the peaks in the absorption and reflection spectra respectively.

In figure 2 the x-ray reflectivity spectra (right-hand part) and the absorption coefficients (left-hand part) of Si crystal near the Si $L_{2,3}$ absorption edge are presented. The details of the permittivity calculation are described in section 4. The glancing angle is $\Theta = 20^\circ$. Both the reflectivity spectra and the absorption coefficients are convoluted with the Lorentz apparatus function, of widths 0.2 eV (upper curves), 0.5 eV (middle curves) and 1.0 eV (lowest curves). One can see from figure 2 that in the x-ray reflectivity spectra the excitonic peak is more distinguishable than in the absorption ones. The absorption spectra in figure 2 correspond to the photocurrent technique (see section 2). Both the transmission and fluorescence techniques provide worse contrast than the photocurrent technique (see figure 1). Figure 2 shows that the XRFS spectrum might be a very sensitive tool for the detection of the existence of excitons.

4. The XRFS spectrum of Si crystal near the Si $L_{2,3}$ edge

Si crystal has the diamond-like structure and therefore its permittivity is isotropic. In the near-edge region the permittivity $\varepsilon(\omega)$ has the form [15, 16] $\varepsilon = 1 - 4\pi nc^2 r_0(f_{norm}^* + f_{anom}^*)/\omega^2$, where $f_{norm}(\omega)$ is the normal part of the atomic scattering factor (ASF) which corresponds to the excitation of all electrons but 2p electrons, $f_{anom}(\omega)$ is the anomalous part of the ASF which is caused by the excitation of the 2p electrons to the valence band, n is the concentration of atoms, ω is the photon frequency, r_0 is the classical electron radius, c is the light velocity, the star means complex conjugation. The imaginary part of f_{norm} above the $L_{2,3}$ absorption edge has been obtained by the extrapolation of atomic data [17]. The real part of f_{norm} in the first approximation [17] has been chosen to be equal to 4 (the number of the electrons in the atom with binding energy less than the energy of the $L_{2,3}$ edge). The calculations of the anomalous parts f_{anom} for Si crystal have been carried out according to the method suggested in reference [16]. The system of the linear equations [18] for the 87-atom cluster (seven coordination spheres) has been solved. The angular momenta up to $l = 2$ for all atoms have

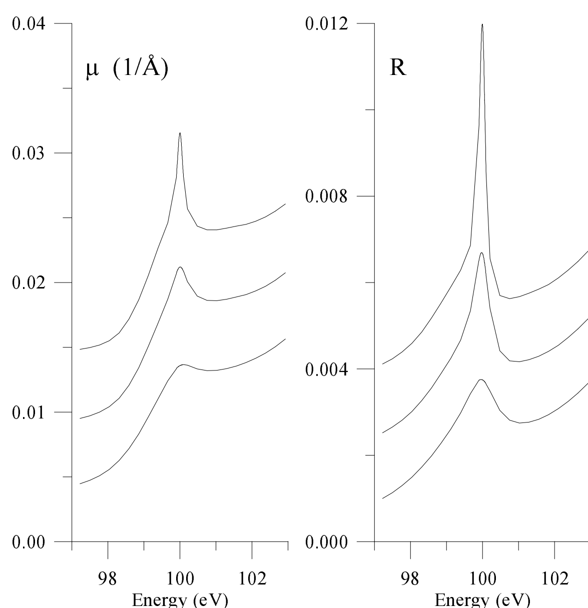

Figure 2. The convoluted absorption coefficient (left-hand part) and the reflectivity (right-hand part) of Si crystal near the Si $L_{2,3}$ absorption edge. The glancing angle (right-hand part) $\Theta = 20^\circ$. The curves correspond to the different widths of the apparatus function Γ_0. The upper curves (both left-hand and right-hand parts) correspond to $\Gamma_0 = 0.2$ eV, the middle curves to $\Gamma_0 = 0.5$ eV and the lowest curves to $\Gamma_0 = 1.0$ eV. For clarity the curves are shifted.

been taken into account. The Herman–Skillman algorithm [19] with the exchange parameter chosen according to Schwarz [20] has been employed to calculate the atomic wave functions. The atomic sphere radii in the cluster are 1.17 Å. Outside the cluster, the potential has been chosen to be equal to the averaged interstitial potential [21]. To include the p-hole presence and the extra-atomic relaxation we have calculated the potential of the ionized Si atom for the configuration $1s^2 2s^2 2p^5 3s^2 3p^3$. To take into consideration the influence of the filled electron states, we have subtracted (according to reference [16]) an integral over path L, where the path L envelops the energies of all the filled electron states with s and d symmetry around the ionized atom. An analogous approach was successfully used to describe the reflectivity of both the hexagonal boron nitrogen crystal near the B K absorption edge [22] and the $PbTiO_3$ crystal near the Ti K absorption edge [23].

The experimental Si $L_{2,3}$ reflectivity spectrum [11, 12] of Si crystal shows a narrow peak near the absorption edge. All our attempts to obtain this prominent feature using the full multiple-scattering method were unsuccessful. But our calculations with and without the 2p hole show that the peak in the absorption spectrum near the bottom of the conduction band has a narrower and sharper form if the 2p hole is taken into account. Thus in the case of the infinite cluster this peak might correspond to the exciton. The observation of the core-exciton state in Si crystal was reported earlier [7]. The excitonic effect within the conduction band has been considered to explain the x-ray absorption data [8].

Let us note that the goal of this paper is not to prove the excitonic origin of the peak by rigorous *ab initio* calculation. Our main aim is to show the possible superiority of the XRFS spectrum for the detection of excitons. To do this one needs a model permittivity which describes reality well, qualitatively. To model the exciton we have subtracted from the

real and imaginary parts of the permittivity the wide peak with small integral intensity (see equations (4) and (3)) with the centre at $E_0 = 100$ eV. After this we added a narrow peak of the same integral intensity. The width of the excitonic peak has been suggested [9] to be $\Gamma_{ex} = 0.01$ eV. Thus we do not change the sum rule—only the peak width. The integral intensity of this peak, expressed as the ASF in the asymptotic region $E \gg E_0$, corresponds to the scattering by 0.01 of the free classical electron. Let us mention that the total anomalous ASF of the 2p shell equals 6 (if $E \gg E_0$). Figure 3 shows the calculated x-ray reflectivity fine structure of Si crystal near the Si $L_{2,3}$ absorption edge. The spectrum is convoluted with the apparatus function of width $\Gamma_0 = 0.1$ eV. The glancing angle is $\Theta = 4^\circ$. While our model has no physical significance, it leads to a good qualitative agreement with the experimental reflectivity spectrum [11]. Therefore it can be used as a tool for probing the validity of the different methods mentioned above.

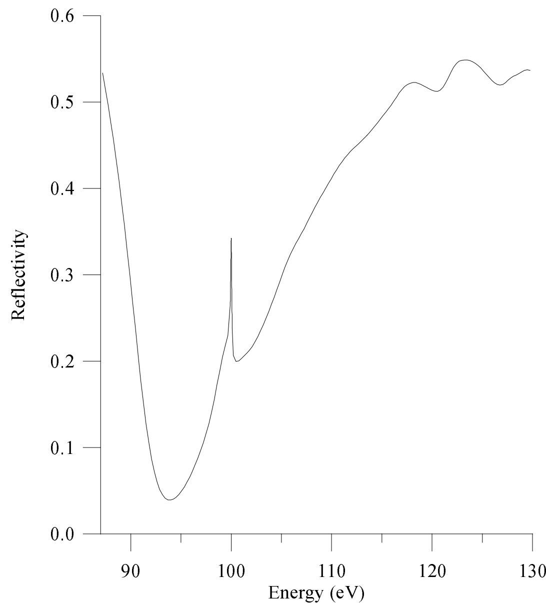

Figure 3. The calculated reflectivity fine-structure spectrum of Si crystal near the Si $L_{2,3}$ absorption edge. The glancing angle $\Theta = 4^\circ$. The width of the apparatus function is 0.1 eV.

5. Conclusions

In this paper we have compared the requirements on the energy resolution of the x-ray transmission, fluorescence, photocurrent and reflectivity techniques for the detection of excitons. The integral intensity of the narrow peak in the reflectivity spectrum is found to be inversely proportional to the width of the peak in the absorption spectrum. Therefore the narrow (excitonic) peak with the small integral intensity could be distinguished much more easily in the x-ray reflectivity spectrum. Using the model permittivity of Si crystal near the $L_{2,3}$ absorption edge we have shown that the x-ray reflectivity technique appears to be the most suitable one for the detection of the excitonic peak. It is found that the assumption of the presence of excitons in Si crystal can explain the narrow peak in the Si $L_{2,3}$ reflectivity spectrum.

Acknowledgment

This work was supported by The Aaron Gutwirth Foundation, Allied Investments Limited (Israel).

References

[1] Altarelli M and Dexter D L 1972 *Phys. Rev. Lett.* **29** 1100
[2] Elliott R J 1957 *Phys. Rev.* **108** 1384
[3] Eberhardt W, Kalkoffen G, Kunz C, Aspnes D and Cardona M 1978 *Phys. Status Solidi* **88** 135
[4] Bauer R S, Bacgrach R Z, McMenamin J C and Aspnes D E 1977 *Nuovo Cimento* B **39** 409
[5] Margaritondo G and Rowe J E 1977 *Phys. Lett.* A **59** 464
[6] Brown F C 1980 *Synchrotron Radiation Research* ed H Winick and S Doniach (New York: Plenum) p 86
[7] Carson R D and Schnatterly S E 1987 *Phys. Rev. Lett.* **59** 319
[8] Bianconi A, Del Sole R, Selloni A, Chiaradia P, Fanfoni M and Davoli I 1987 *Solid State Commun.* **64** 1313
[9] Rubensson J-E, Mueller D, Shuker R, Ederer D L, Zhang C H, Jia J and Callcott T A 1990 *Phys. Rev. Lett.* **64** 1047
[10] Blossey D 1971 *Phys. Rev.* B **3** 1382
[11] Vinogradov A S, Filatova E O and Zimkina T M 1982 *Sov. Phys.–Solid State* **24** 979
[12] Filatova E, Stepanov A, Blessing C, Friedrich J, Barchewitz R, André J-M, Le Guern F, Bac S and Troussel P 1995 *J. Phys.: Condens. Matter* **7** 2731
[13] Lee P A 1976 *Phys. Rev.* B **13** 526
[14] Citrin P H, Eisenberger P and Hewitt R C 1978 *Phys. Rev. Lett.* **15** 449
[15] James R W 1958 *The Optical Principles of the Diffraction of X-rays* (London: Bell)
[16] Vedrinskii R V, Kraizman V L, Novakovich A A and Machavariani V Sh 1992 *J. Phys.: Condens. Matter* **4** 6155
[17] Henke B L, Gullikson E M and Davis J C 1993 *At. Data Nucl. Data Tables* **54** 181
[18] Ashley C A and Doniach S 1975 *Phys. Rev.* B **11** 1279
Vedrinskii R V and Novakovich A A 1975 *Fiz. Met. Metalloved.* **39** 7 (Engl. Transl. 1975 *Phys. Met. Metallogr.* **39** 1)
[19] Herman F and Skillman S 1963 *Atomic Structure Calculation* (Englewood Cliffs, NJ: Prentice-Hall)
[20] Schwarz K 1972 *Phys. Rev.* B **5** 2466
[21] Doniach S, Berding M, Smith T and Hodgson K O 1984 *EXAFS and Near Edge Structure III* ed K O Hodgson, B Hedman and J E Penner-Hahn (Berlin: Springer) p 33
[22] Vedrinskii R V, Kraizman V L, Novakovich A A and Machavariani V Sh 1993 *J. Phys.: Condens. Matter* **5** 8643
[23] Vedrinskii R V, Novakovich A A, Kraizman V L, Bermous A G and Machavariani V Sh 1995 *Physica* B **208+209** 11